

CASE FILE
COPY

NASA MEMO 2-3-59A

NASA MEMO 2-3-59A

11-05
2/4/64

NASA

MEMORANDUM

AN EXPERIMENTAL INVESTIGATION OF A TRIANGULAR WING
OF ASPECT RATIO 2 AND A BODY WARPED TO BE

TRIMMED AT $M = 2.24$

By Gaynor J. Adams and John W. Boyd

Ames Research Center
Moffett Field, Calif.

Declassified March 15, 1962

NATIONAL AERONAUTICS AND SPACE ADMINISTRATION

WASHINGTON

February 1959



NATIONAL AERONAUTICS AND SPACE ADMINISTRATION

MEMORANDUM 2-3-59A

AN EXPERIMENTAL INVESTIGATION OF A TRIANGULAR WING
OF ASPECT RATIO 2 AND A BODY WARPED TO BE
TRIMMED AT $M = 2.24$

By Gaynor J. Adams and John W. Boyd

SUMMARY

A cambered and twisted triangular wing of aspect ratio 2 in combination with a cambered body was investigated experimentally to determine the effectiveness of the camber in reducing the drag due to lift at trim at supersonic speeds. Four arrangements were tested comprising all combinations of a symmetrical and a cambered wing with a symmetrical and a cambered body. The camber shape investigated was derived by linearized lifting surface theory for triangular wings with sonic leading edges and satisfied the requirement that the wing be trimmed at the design Mach number and lift coefficient.

The experimental results for the cambered wing and cambered body showed that the drag coefficient at trim was always greater, at the same lift coefficient, than that for the untrimmed symmetrical wing and body. The trim lift coefficient was positive and decreased with increasing Mach number. At the design Mach number of 2.24, the trim lift coefficient was somewhat lower and the drag coefficient was higher than values predicted by linearized lifting surface theory for the wing alone.

A comparison of the trim lift-drag ratio of the cambered wing and cambered body with values obtained by trimming the symmetrical wing and symmetrical body either with a canard or a trailing-edge flap showed that, at approximately the design Mach number, the cambered configuration developed a somewhat higher value than the trailing-edge flap configuration but a lower value than the canard configuration.

INTRODUCTION

The problem of efficient flight at supersonic speeds has placed great emphasis on the attainment of high lift-drag ratios. In order to achieve this goal numerous theoretical and experimental studies (see refs. 1 through 7) have been undertaken to reduce the drag due to lift of an aircraft. A large part of the drag associated with flight at these speeds may be due to trimming the aircraft. An investigation was undertaken, therefore, to design and test a wing with reduced drag due to lift at trim at supersonic Mach numbers.

The initial part of the investigation was directed at determining a mean-surface shape for triangular wings with sonic leading edges which would provide trim at a specified lift coefficient while at the same time approximating the drag due to lift of a symmetrical triangular wing. It is the purpose of the present report to present experimental results for a wing constructed according to these conditions, with a brief discussion of the design method. A cambered and twisted triangular wing of aspect ratio 2 mounted on a cambered Sears-Haack body was tested for this purpose. Additional tests were conducted with the cambered wing mounted on a symmetrical body, and a symmetrical wing mounted on the symmetrical or the cambered body. A comparison of the theoretical wing-alone drag polar and the measured polar for the cambered wing and cambered body is made at the design Mach number. Additional data on the effectiveness of trimming a symmetric triangular wing and body by means of a canard and a trailing-edge flap are presented for comparison.

SYMBOLS

a_{ij}	multiplying constant associated with the elementary pressure distribution, $\left(\frac{\Delta p}{q}\right)_{ij}$
b	wing span
C_D	drag coefficient, $\frac{\text{drag}}{qS}$
$C_{D_{ij}}$	drag-due-to-lift coefficient for the pressure distribution, $\left(\frac{\Delta p}{q}\right)_{ij}$
$C_{D_{ij,rs}}$	interference drag coefficient between pressure distributions, $\left(\frac{\Delta p}{q}\right)_{ij}$ and $\left(\frac{\Delta p}{q}\right)_{rs}$

C_L	lift coefficient, $\frac{\text{lift}}{qS}$
$C_{L_{ij}}$	lift coefficient for the pressure distribution, $\left(\frac{\Delta p}{q}\right)_{ij}$
C_m	pitching-moment coefficient, $\frac{\text{pitching moment}}{qS\bar{c}}$, referred to the 0.35 point of the mean aerodynamic chord
$C_{m_{ij}}$	pitching-moment coefficient for the pressure distribution, $\left(\frac{\Delta p}{q}\right)_{ij}$
\bar{c}	mean aerodynamic chord
c_r	root chord
$\frac{L}{D}$	lift-drag ratio
M	free-stream Mach number
$\left(\frac{\Delta p}{q}\right)_{ij}$	lifting-pressure coefficient, $\left(\frac{x}{c_r}\right)^i \left \frac{y}{s_0}\right ^j$
q	free-stream dynamic pressure
R	Reynolds number, based on the mean aerodynamic chord
S	wing area, including part inside the body
s_0	wing semispan, root chord to tip
x, y, z	Cartesian coordinates in streamwise, spanwise, and vertical directions, respectively
z_{ij}	surface ordinate of wing mean camber surface with pressure distribution, $\left(\frac{\Delta p}{q}\right)_{ij}$
α	angle of attack of body nose, deg

α_{ij}	local angle of attack in radians of wing with pressure distribution, $\left(\frac{\Delta p}{q}\right)_{ij}$
β	$\sqrt{M^2-1}$
Δp	difference between local pressures on lower and upper surfaces of wing
μ	$\frac{y}{x}$

Subscripts

i, j, r, s summation subscripts (positive integers, ≥ 0)

APPARATUS

Test Facilities

The experimental data were obtained in the Ames 6- by 6-foot supersonic wind tunnel and the 8- by 7-foot test section of the Ames Unitary Plan wind tunnel. The 6- by 6-foot wind tunnel is a closed-circuit variable-pressure type with a Mach number range continuous from 0.70 to 2.24. The tunnel floor and ceiling have perforations to permit transonic testing. A somewhat more detailed description of this tunnel may be found in reference 8. The Unitary Plan wind tunnel is also a closed-circuit variable-pressure type and the 8- by 7-foot test section has a Mach number range continuous from 2.5 to 3.5. A more detailed description of the tunnel may be found in reference 9.

In both wind tunnels the models were sting-mounted and the forces and moments measured with a six-component internal strain-gage balance.

Models

Design conditions and procedures.- The present research investigated the effectiveness of camber and twist in reducing the supersonic drag due to lift at trim for a triangular wing of aspect ratio 2. To derive a lifting surface which will achieve a low drag due to lift in trimmed flight, two conditions must be satisfied simultaneously, the surface must support a specified total lift and the center of pressure of this lift must be located so as to give zero pitching moment about a given center of moments. For the present wing which was designed for a Mach number

of 2.24 (sonic leading edge) the design lift coefficient was 0.20 and the center of pressure was at the 0.35 point of the wing mean aerodynamic chord. It was estimated that placing the center of moments at this position would provide a static margin of approximately $0.05\bar{c}$ at subsonic speeds.

The camber shape to satisfy these conditions was derived from linearized theory by superposition of a number of surfaces having finite pressure distributions (see refs. 4 and 7). Each of the elementary loads was multiplied by an arbitrary constant whose magnitude determined the contribution of each load to the total pressure distribution. The constants were evaluated by means of the standard minimization procedures (ref. 10) for the condition of minimum drag with a given lift and pitching moment. The surface shape and the total forces and moments were then obtained.

The form of the individual pressures used in the superposition process is

$$\left(\frac{\Delta p}{q}\right)_{ij} = \left(\frac{x}{c_r}\right)^i \left|\frac{y}{s_0}\right|^j \quad (1)$$

where i and j are positive integers. This expression is multiplied by arbitrary constants a_{ij} and the total lifting-pressure coefficient is given by the sum

$$\left(\frac{\Delta p}{q}\right) = \sum_{i,j} a_{ij} \left(\frac{\Delta p}{q}\right)_{ij} \quad (2)$$

It should be noted here that only certain values of i and j were used to obtain the pressure distribution. The angle-of-attack distributions α_{ij} corresponding to the loadings $(\Delta p/q)_{ij}$ have singularities on the root chord for $i = j = 0$ and $i = 0, 1, 2, 3, \dots, j = 1$. Omitting these loads from the series and expanding equation (2) for $i + j \leq 3$ yield

$$\begin{aligned} \frac{\Delta p}{q} = & a_{10} \left(\frac{x}{c_r}\right) + a_{20} \left(\frac{x}{c_r}\right)^2 + a_{02} \left(\frac{y}{s_0}\right)^2 + a_{30} \left(\frac{x}{c_r}\right)^3 + \\ & a_{03} \left|\frac{y}{s_0}\right|^3 + a_{12} \left(\frac{x}{c_r}\right) \left(\frac{y}{s_0}\right)^2 \end{aligned} \quad (3)$$

The drag coefficient corresponding to each elementary load is given by

$$C_{Dij} = \frac{1}{S} \int \left(\frac{\Delta p}{q}\right)_{ij} \alpha_{ij} dS \quad (4)$$

and the interference drag coefficient between two loadings $(\Delta p/q)_{ij}$

and $(\Delta p/q)_{rs}$ is given by

$$C_{D_{ij,rs}} = \frac{1}{S} \int \left[\left(\frac{\Delta p}{q} \right)_{ij} \alpha_{rs} + \left(\frac{\Delta p}{q} \right)_{rs} \alpha_{ij} \right] dS \quad (5)$$

where r and s are also positive integers. The total drag coefficient corresponding to the loading $(\Delta p/q)$ for any values of the constants a_{ij} is given by

$$C_D = \sum_{i,j} a_{ij}^2 C_{D_{ij}} + \frac{1}{2} \sum_{ij,rs} a_{ij} a_{rs} C_{D_{ij,rs}}; \quad i,j \neq r,s \quad (6)$$

The total lift and pitching-moment coefficients are given by

$$C_L = \sum_{i,j} a_{ij} C_{L_{ij}} \quad (7)$$

$$C_m = \sum_{i,j} a_{ij} C_{m_{ij}} \quad (8)$$

It is possible by application of standard minimization procedures (see ref. 10) to equations (6), (7), and (8), for the conditions of minimum drag with given lift and pitching moment, to obtain a set of linear simultaneous equations to be solved for the values of the constants a_{ij} .

The final surface shape or angle-of-attack distribution is then given as

$$\alpha = \sum a_{ij} \alpha_{ij} \quad (9)$$

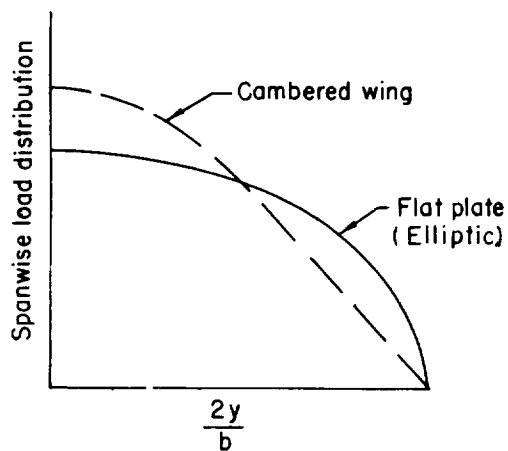
where a_{ij} are the constants as obtained in the above optimization procedure. The surface slopes, ordinates, and drag coefficients corresponding to each of the elementary loads used are given in the appendix. The minimum value of the drag-due-to-lift factor for the loading given by equation (3), for given lift and location of the center of pressure at the 0.35 point of the mean aerodynamic chord, is $C_D/\beta C_L^2 = 0.269$,¹ or 8 percent above the value for an untrimmed symmetrical wing. This value is 40 percent below the theoretical value for a symmetrical wing and symmetrical body trimmed with straight trailing-edge flaps having an exposed area equal to 11 percent of the total wing area.

¹The addition of fourth degree terms to the six-term series resulted in negligible changes in drag due to lift and surface shape.

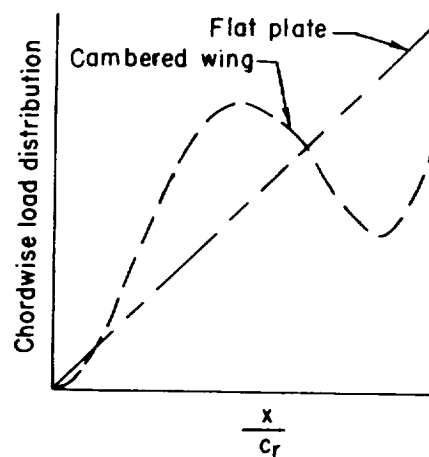
The linearized lifting surface theory relates only the streamwise slope of the surface to the loading. Thus, an arbitrary function of the spanwise coordinate y may be added to the equation for the ordinate of any lifting surface. In the present case, the arbitrary function of y was chosen so that the wing trailing edge was straight. Ordinates of the resulting mean camber surface at several spanwise stations and of the leading- and trailing-edge traces are shown in figure 1 for the wing alone.

To provide for the presence of the body, that portion of the cambered surface of the wing covered by the body was altered so as to be cambered only in the streamwise direction and flat in the lateral direction. The ordinates of this strip, which passed through the trailing edge, were then calculated by specifying that the total chordwise loading on the surface consisting of the strip and the part of the cambered wing outside the body be the same as that on the cambered wing alone. On the assumption that the effect of the body on the total lift and moment characteristics would be the same as that of the zero-thickness strip, the ordinates of the strip were used as the ordinates of the body axis. The effect of this assumption on the drag is not known, but was assumed to be small.

The spanwise and chordwise loadings for the cambered wing alone and the plane wing are shown in sketches (a) and (b), respectively. The comparison of chordwise loadings is of interest in that it shows the forward distribution of the loading on the cambered wing which produces the trimming moment.



Sketch (a)



Sketch (b)

Description of models.— Four wing-body configurations were investigated, consisting of the combinations of a symmetrical wing or a cambered wing with a symmetrical body or a cambered body. A photograph of the cambered wing-body configuration is shown in figure 2, and dimensional sketches of the four models are shown in figure 3.

Both of the wings had triangular plan forms of aspect ratio 2 and the NACA 0003-63 thickness distribution in the streamwise direction. The symmetrical Sears-Haack body had a fineness ratio 12.5 with the afterportion removed, as shown in figure 3, to accommodate the sting and balance. The cambered body had a fineness-ratio-12.5 Sears-Haack radius distribution about an axis which was cambered in the region of the wing as described in the previous section. The center line of the body ahead of the wing apex was straight, and was used as the reference axis for the body. The afterportion of the cambered body was removed to accommodate the sting and balance.

The symmetrical and cambered wings could be mounted interchangeably on the symmetrical and cambered bodies. The slot into which the wings were inserted in the cambered body was cut at an angle of 9.7° with respect to the reference axis in order to fit the existing balance into the body. Thus, when the cambered wing is mounted on the symmetrical body, the angle of attack of the wing is reduced 9.7° below that for the design attitude, and the wing lift is negative at zero body incidence.

The results for configurations employing a trailing-edge flap and a canard control, with which the present data will be compared, made use of the above described symmetrical wing and symmetrical body.² The trailing-edge flap was a full-span control whose exposed area was 10.7 percent of the total wing area. The canard had an aspect-ratio-2 triangular plan form with an exposed area of 6.9 percent of the total wing area. The experimental results for the canard configuration have been published in references 11 and 12; reference 13 presents an analysis of these and other canard data.

TEST AND PROCEDURES

Range of Test Variables

Mach numbers of 0.70, 0.90, 1.00, 1.10, 1.30, 1.70, 2.22, 2.24, 2.58, 3.06, and 3.53 and angles of attack ranging from -17° to $+19^\circ$ were covered in the investigation. Results were not obtained, however, for the symmetrical wing and cambered body at Mach numbers above 2.22. The test Reynolds number based on the wing mean aerodynamic chord was 3.68 million, except for the symmetrical wing-body at $M = 1.00$ and 1.10, where it was 1.84 million. For test Mach numbers below 2.58 wires of 0.010-inch diameter were placed on the wings and bodies at the locations shown in figure 3 to induce transition. No wires were placed on the models for tests at Mach numbers of 2.58 and above, since the wire size required to induce transition results in excessive pressure drag.

²All trailing-edge flap data used in this report are from unpublished results obtained in the Ames 6- by 6-foot supersonic wind tunnel. All statements made in the section Test and Procedures in this report apply to the trailing-edge flap data, as well as to the data included herein.

Reduction of Data

The data presented herein have been reduced to standard coefficient form. The pitching-moment coefficients have been referred to the projection of the 0.35 point of the mean aerodynamic chord on the balance center line. For each configuration the angle of attack was referred to the reference axis of the body. The results have been adjusted to take account of the following effects:

Base drag.- The base pressure was measured and the drag data were adjusted to correspond to a base pressure equal to the free-stream static pressure.

Stream inclination.- The data obtained in the Ames 6- by 6-foot supersonic wind tunnel were corrected for a stream angle inclination of less than 0.30° , which existed through the Mach number range of the tests. Similar corrections were made for the data obtained in the 8- by 7-foot test section of the Ames Unitary Plan wind tunnel, where the stream angle inclination was less than 0.21° over the range of test Mach numbers.

Model buoyancy.- The drag data obtained in the 8- by 7-foot test section include buoyancy corrections due to longitudinal static-pressure variations in the vicinity of the model. These corrections amounted to less than 1.6 percent of the zero lift drag of the uncambered model.

Tunnel-wall interference.- Previous experiments made in the perforated test section of the Ames 6- by 6-foot tunnel at transonic and subsonic Mach numbers have shown that no corrections for wall interference are required (see ref. 8).

RESULTS AND DISCUSSION

The primary purpose of the present investigation was to evaluate the effectiveness of the distributed camber derived herein in reducing the drag at trim of a triangular-wing configuration at supersonic speeds. The calculations showed that, for triangular wings with sonic leading edges incorporating this camber, the drag due to lift in the trimmed attitude could approach the drag-due-to-lift value of the untrimmed symmetrical wing. The various combinations of symmetrical and cambered wing and symmetrical and cambered body were tested; all of the results are presented in tabular form in tables I through IV. Representative plots of the basic lift, drag, and pitching-moment characteristics are presented in figure 4 over a Mach number range from 0.90 to 3.53 for all of the models tested. A comparison of the experimental characteristics for the cambered wing and cambered body model with the predicted

wing-alone values is shown in figure 5 at the design Mach number of 2.24. To assess the trim characteristics of the cambered wing a comparison is made in figures 6 and 7 with the trim lift-drag ratio of the symmetrical configuration trimmed with a trailing-edge flap and with a canard control.

Basic Data

Examination of the data of figure 4 which compare the results for the four configurations tested shows several points of interest. The results for the cambered wing and cambered body show that the configuration trims at a positive lift coefficient throughout the Mach number range investigated. Further, the lift coefficient at which trim occurs steadily increases with decreasing Mach number from a value of 0.135 at a Mach number of 3.53 to 0.73 at a Mach number of 0.90. The results show also that at the lift coefficient corresponding to trim conditions for the cambered wing and body, the drag coefficient of the cambered configuration is always greater than that for the symmetrical wing untrimmed. A point of further significance is that at lift coefficients below trim at supersonic speeds the drag due to camber is large and would impose penalties on the performance of an aircraft utilizing this type of camber if it had to fly at lifts below the design value.

The results for the cambered wing tested on the symmetrical body show also that this configuration was trimmed at Mach numbers up to 2.22. The data show further that the trimmed attitude is attained with less drag than that for the cambered wing and body at the same lift coefficient. At the higher Mach numbers the gradual reduction in pitching-moment curve slope, dC_m/dC_L , with increasing lift coefficient prevented the attainment of a trim condition. This slope change probably results from the larger unstable moment associated with the lift acting over the forward part of the body, since for a given lift coefficient the forward portion of the body is at a considerably higher angle of attack for the cambered wing and symmetrical body than for the cambered wing and cambered body.

It is of interest to make a comparison of the experimental characteristics of the cambered wing and body with those predicted for the wing alone at the design Mach number of 2.24. This comparison is shown in figure 5 where the theoretical wing-alone characteristics for both the cambered and the symmetrical wings are shown. It is evident that the cambered wing and body does not trim at a lift coefficient as high as the predicted value nor does it realize as low a drag coefficient as was predicted. It is interesting to note, however, that at lift coefficients near zero the large increment in drag due to camber is in good agreement with the theory.

The high values of the experimental drag coefficient at the trim attitude may be associated in part with viscous separation effects similar to that noted on the cambered wing of reference 6. The local slopes of the wing surface inboard of 0.30 of the wing semispan are as high as 14° , and the attainment of the linear-theory values of lift and drag cannot be expected. Some lack of agreement between theory and experiment is evident even in the results of the symmetrical configuration of figure 5 at moderate angles of attack, where the results show a lower lift and higher drag than predicted by the theory. Wing-body interference effects on lift-curve slope can only account for a part of this difference for the symmetrical wing and body. These interference effects are not known for the cambered configuration but probably also contribute to the measured drag values being higher than those predicted.

Lift-Drag Ratios

The foregoing results have shown that the cambered wing and body fell short of the theoretical expectations. It is of interest, however, to compare the drag due to trimming a triangular wing and body by means of camber and twist with that due to trimming with control surfaces such as trailing-edge flaps or canards. This comparison may be seen from figure 6 which presents the lift-drag ratio as a function of lift coefficient for a triangular wing and body trimmed by these three means at several Mach numbers. It should be noted that the configurations utilizing either a flap or a canard are trimmed throughout the lift-coefficient range whereas the cambered wing and body is trimmed only at the lift coefficient noted in the figure. The static margin of all three at a Mach number of 0.70 was chosen to be that obtained experimentally for the cambered configuration at that Mach number (0.06c). Experimental data for the wing trimmed with a trailing-edge flap were not available at Mach numbers above 2.22.

The results show no improvement in lift-drag ratio at subsonic speeds through the use of this camber. At a Mach number of 1.30 the trimmed lift-drag ratio of the cambered configuration was about the same as the maximum lift-drag ratio of the wing trimmed with a flap. However, the trimmed attitude of the cambered wing occurred at a considerably higher lift coefficient than the optimum lift coefficient of the trailing-edge flap wing with the result that at the lift coefficient where the cambered wing was trimmed its lift-drag ratio was considerably higher than that of the configurations trimmed with either a trailing-edge flap or a canard. At a Mach number of 2.22, which was approximately the design condition, the results show that the trimmed lift-drag ratio of the cambered wing is only slightly greater than the maximum trimmed lift-drag ratio of the flap-trimmed wing and somewhat less than that for the configuration trimmed with the canard. Here as at a Mach number of 1.3, the cambered wing and body trimmed at a lift coefficient greater than the optimum lift

coefficient of either of the other two configurations. A point of interest here is that, unlike the results at a Mach number of 1.3 where the trim lift occurred at a point considerably above the optimum lift coefficient, the cambered wing was trimmed at the optimum lift coefficient. At the two higher Mach numbers of 3.06 and 3.53 the wing and body trimmed with the canard realized a higher maximum lift-drag ratio than did the cambered configuration.

One other point of interest can be seen from the results of figure 7 which compares the trim characteristics of the three configurations discussed in figure 6 with those of the cambered wing and symmetrical body at a Mach number of 2.22. The results show that the cambered wing and symmetrical body had a higher maximum lift-drag ratio than did the cambered wing and body. However, at maximum lift-drag ratio the cambered wing and symmetrical body was untrimmed whereas the cambered wing and body was nearly trimmed. An examination of the data for symmetric wing-body configurations (of refs. 11 and 12) indicates, however, that the cambered wing and symmetrical body used in conjunction with a canard control for trim at lift coefficients below 0.25, the trim point of the cambered wing, could develop higher trimmed lift-drag ratios than the cambered wing and body. (It should be noted that the characteristics of the controls in combination with the cambered wing and symmetrical body were obtained by superposition of the test data.) For example, the cambered wing and symmetrical body could be trimmed with a canard at a lift coefficient of 0.16 with a maximum lift-drag ratio of 5.7 as compared with a maximum trimmed value of 5.4 for the cambered wing and cambered body. This, of course, indicates that the body camber used herein is not necessary or desirable to obtain the best trim characteristics. However, as can be seen from the results, the symmetrical configuration trimmed with a canard develops a higher maximum trimmed lift-drag ratio than does either of the configurations having the cambered wing.

SUMMARY OF RESULTS

An experimental investigation was made to determine the effectiveness of camber in reducing the drag at trim of a triangular wing of aspect ratio 2 at supersonic speeds. The results of the investigation showed:

1. The drag coefficient of the cambered wing and body at trim was always greater than the value for the untrimmed symmetrical wing and body at the same lift coefficient. The cambered wing-body configuration trimmed at a positive lift coefficient at all Mach numbers, the value of the trim lift coefficient decreasing with increasing Mach number.

2. At the design Mach number of 2.24 the cambered wing trimmed at a lower lift coefficient and had a higher drag coefficient than predicted.

3. At approximately the design Mach number the cambered wing and body realized a trimmed lift-drag ratio that was slightly greater than the maximum value achieved by the symmetrical configuration trimmed with a trailing-edge flap, and was less than that for the symmetrical configuration trimmed with a canard.

Ames Research Center

National Aeronautics and Space Administration

Moffett Field, Calif., Nov. 4, 1958

APPENDIX

CHARACTERISTICS OF THE ELEMENTARY LOADS $\left(\frac{\Delta p}{q}\right)_{ij}$

For any value of the multiplying factors a_{ij} , the total lift, drag due to lift, and pitching moment corresponding to the loading

$$\frac{\Delta p}{q} = \sum_{ij} a_{ij} \left(\frac{\Delta p}{q}\right)_{ij}$$

where

$$\left(\frac{\Delta p}{q}\right)_{ij} = \left(\frac{x}{c_r}\right)^i \left|\frac{y}{s_0}\right|^j \quad i, j = \text{positive integers} \quad (A1)$$

depend on the lift, drag, and moment coefficients of the elementary loads $(\Delta p/q)_{ij}$. (See eqs. (1) through (8).) For a triangular wing with sonic leading edge and unit root chord and semispan, the surface slopes α_{ij} and ordinates z_{ij} to support these elementary loads at $M = \sqrt{2}$, as given by linear theory, are as follows: ($\mu = y/x$; $i + j \leq 3$; no root singularities in α_{ij})

$$\frac{\alpha_{10}}{x} = \frac{1}{\pi} \sqrt{1-\mu^2}$$

$$\frac{z_{10}}{x^2} = \frac{1}{2\pi} \left[\mu^2 \cosh^{-1} \left| \frac{1}{\mu} \right| - \sqrt{1-\mu^2} \right]$$

$$\frac{\alpha_{20}}{x^2} = \frac{1}{2\pi} \left[\mu^2 \cosh^{-1} \left| \frac{1}{\mu} \right| + \frac{5}{3} \sqrt{1-\mu^2} \right]$$

$$\frac{z_{20}}{x^3} = \frac{1}{2\pi} \left[\mu^2 \cosh^{-1} \left| \frac{1}{\mu} \right| + \frac{1}{9} (5-14\mu^2) \sqrt{1-\mu^2} \right]$$

$$\frac{\alpha_{02}}{x^2} = \frac{1}{2\pi} \left[3\mu^2 \cosh^{-1} \left| \frac{1}{\mu} \right| - \frac{1}{3} \sqrt{1-\mu^2} \right]$$

$$\frac{z_{02}}{x^3} = \frac{1}{2\pi} \left[-3\mu^2 \cosh^{-1} \left| \frac{1}{\mu} \right| + \frac{1}{9} (1+26\mu^2) \sqrt{1-\mu^2} \right]$$

$$\frac{\alpha_{30}}{x^3} = \frac{4}{5\pi} \left[(1+\mu^2) \sqrt{1-\mu^2} \right]$$

$$\frac{z_{30}}{x^4} = \frac{1}{5\pi} \left[\frac{5}{2}\mu^4 \cosh^{-1} \left| \frac{1}{\mu} \right| - \left(1 + \frac{3}{2} \mu^2 \right) \sqrt{1-\mu^2} \right]$$

$$\frac{\alpha_{03}}{x^3} = \frac{-1}{4\pi} \left[6\mu^2 \cosh^{-1} \left| \frac{1}{\mu} \right| + \frac{2}{15} (1-94\mu^2) \sqrt{1-\mu^2} \right]$$

$$\frac{z_{03}}{x^4} = \frac{1}{4\pi} \left[\left(3\mu^2 + \frac{19}{4} \mu^4 \right) \cosh^{-1} \left| \frac{1}{\mu} \right| + \left(\frac{1}{30} - \frac{467}{60} \mu^2 \right) \sqrt{1-\mu^2} \right]$$

$$\frac{\alpha_{12}}{x^3} = \frac{4}{45\pi} \left[(19\mu^2-1) \sqrt{1-\mu^2} \right]$$

$$\frac{z_{12}}{x^4} = \frac{1}{90\pi} \left[75\mu^4 \cosh^{-1} \left| \frac{1}{\mu} \right| + (2-77\mu^2) \sqrt{1-\mu^2} \right]$$

For $M \neq \sqrt{2}$, the right side of the above equations for α_{ij} and z_{ij} should be multiplied by β ; z_{ij} should be replaced by z_{ij}/c_r ; and μ replaced by $\beta y/x$.

The lift and moment coefficients of the elementary loads can be easily obtained by integration of equation (A1).

The drag coefficients are given in the following table:

ij	$C_{D_{ij}}$	ij	rs	$C_{D_{ij,rs}}$
10	0.125000	10	20	0.200000
20	.0833333	10	02	.0583333
02	.015278	10	30	.166667
30	.062500	10	03	.034980
03	.008034	10	12	.048611
12	.011806	20	02	.051389
		20	30	.142857
		20	03	.032004
		20	12	.044048
		02	30	.045238
		02	03	.021414
		02	12	.026587
		30	03	.028964
		30	12	.039583
		03	12	.019192

For $M \neq \sqrt{2}$, these values should be multiplied by β .

For calculating the drag characteristics at lift coefficients other than the design lift, the interference drags between the elementary loads and the plane wing loading are required. The interference drag is given by

$$C_{D_{p,ij}} = \frac{1}{S} \int \left[\left(\frac{\Delta p}{q} \right)_p \alpha_{ij} + \left(\frac{\Delta p}{q} \right)_{ij} \alpha_p \right] dS$$

$$\equiv d_{p,ij} C_{L_p} C_{L_{ij}}$$

where

$\left(\frac{\Delta p}{q} \right)_p, \alpha_p$ plane wing lifting pressure coefficient and angle of attack, respectively

C_{L_p} plane wing lift coefficient

For $i + j \leq 3$, the interference drag factors $d_{p,ij}$ are as follows:

<u>ij</u>	<u>$d_{p,ij}$</u>
10	0.452642
20	.461014
02	.527998
30	.466152
03	.156382
12	.538202

For $M \neq \sqrt{2}$, these values should be multiplied by β .

REFERENCES

1. Jones, R. T.: Theoretical Determination of the Minimum Drag of Airfoils at Supersonic Speeds. Jour. Aero. Sci., vol. 19, no. 12, Dec. 1952, pp. 813-822. (Also available as IAS preprint 375)
2. Graham, E. W.: A Drag Reduction Method for Wings of Fixed Planform. Jour. Aero. Sci., vol. 19, no. 12, Dec. 1952, pp. 823-825. (Also available as Rep. SM-14441, Douglas Aircraft Co., Santa Monica, July 1952)
3. Tucker, Warren A.: A Method for the Design of Sweptback Wings Warped to Produce Specified Flight Characteristics at Supersonic Speeds. NACA Rep. 1226, 1955. (Supersedes NACA RM L51F08)
4. Grant, Frederick C.: The Proper Combination of Lift Loadings for Least Drag on a Supersonic Wing. NACA Rep. 1275, 1956. (Supersedes NACA TN 3533)
5. Cohen, Doris: The Warping of Triangular Wings for Minimum Drag at Supersonic Speeds. Jour. Aero. Sci. (Readers Forum), vol. 24, no. 1, Jan. 1957, pp. 67-68.
6. Katzen, Elliott D.: Idealized Wings and Wing-Bodies at a Mach Number of 3.0. NACA TN 4361, 1958.
7. Stewart, J. D.: Design of Minimum Drag Mean Surface for Pointed Tip Wing Planforms at Supersonic Speeds - Subsonic Leading Edge and Assumed Loading. Convair Rep. FZA-114, March 12, 1956.
8. Peterson, Victor L., and Boyd, John W.: Effects of Conical Camber on the Lift, Drag, and Pitching-Moment Characteristics of a Triangular Wing of Aspect Ratio 3.0. NACA RM A56L18, 1957.
9. Huntsberger, Ralph F., and Parsons, John F.: The Design of Large High-Speed Wind Tunnels. NACA Paper presented at the Fourth General Assembly of the AGARD Wind Tunnel Panel, Schevenigen, Netherlands, AG15/P6, May 3 - 7, 1954.
10. Sokolnikoff, Ivan S.: Advanced Calculus. McGraw-Hill Book Co., Inc., 1939.
11. Boyd, John W., and Peterson, Victor L.: Static Stability and Control of Canard Configurations at Mach Numbers From 0.70 to 2.22 - Longitudinal Characteristics of a Triangular Wing and Canard. NACA RM A57J15, 1958.

12. Hedstrom, Ernest C., Blackaby, James R., and Peterson, Victor L.:
Static Stability and Control Characteristics of a Triangular Wing
and Canard Configuration at Mach Numbers From 2.58 to 3.53.
NACA RM A58C05, 1958.
13. Hall, Charles F., and Boyd, John W.: Effects of Canards on Airplane
Performance and Stability. NACA RM A58D24, 1958.

TABLE I.- AERODYNAMIC CHARACTERISTICS OF SYMMETRICAL WING AND SYMMETRICAL BODY; $R = 3.58 \times 10^6$
 (EXCEPT AT $M = 1.00$ AND 1.10 WHERE $R = 1.84 \times 10^6$)

Transition wire on													
M	α	C_L	C_D	C_m	M	α	C_L	C_D	C_m	M	α	C_L	C_m
0.70	-6.3	-0.308	0.0379	0.0240	0.90	-6.0	-0.327	0.0406	0.0279	1.00	-5.9	-0.338	0.0484
	-4.3	-0.200	0.0266	0.0199		-4.0	-0.208	0.0213	0.0171		-5.8	-0.212	0.0262
	-2.3	-0.099	0.0117	0.0061		-2.0	-0.097	0.0120	0.0087		-1.8	-0.097	0.0185
	-8	-0.41	0.097	0.053		-5	-0.32	0.097	0.063		-3	-0.21	0.153
	-3	-0.18	0.087	0.048		0	-0.11	0.094	0.051		7	0.031	0.147
	1.7	0.03	0.0091	0.0050		2.0	0.084	0.0107	0.0060		2.1	0.109	0.178
	3.7	0.162	0.0164	0.018		4.0	0.190	0.0202	0.0084		4.1	0.229	0.346
	5.7	0.263	0.0304	0.036		6.0	0.303	0.0369	0.0180		6.2	0.349	0.490
	7.8	0.376	0.0534	0.056		8.0	0.436	0.0657	0.0324		8.2	0.470	0.798
	9.8	0.489	0.0849	0.085		10.0	0.557	0.1008	0.0450		10.2	0.584	1.151
	11.7	0.602	0.1229	0.115		12.0	0.682	0.1475	0.0618		12.1	0.692	1.591
	13.7	0.714	0.1699	0.158		14.0	0.804	0.2018	0.0780		14.2	0.801	2.109
	15.7	0.828	0.2258	0.215		16.0	0.934	0.2694	0.0972		16.2	0.907	2.711
	17.7	0.934	0.2881	0.2810		18.0			0.0999		18.2	0.999	3.351

Transition wire off													
M	α	C_L	C_D	C_m	M	α	C_L	C_D	C_m	M	α	C_L	C_m
1.30	-6.1	-0.287	0.0401	0.0445	1.70	-6.3	-0.236	0.0358	0.0347	2.22	-5.8	-0.174	0.0275
	-4.0	-0.186	0.0227	0.0286		-4.3	-0.162	0.0230	0.0237		-3.8	-0.114	0.0177
	-2.0	-0.087	0.0151	0.0136		-2.2	-0.079	0.0148	0.0120		-1.7	-0.050	0.0122
	-5	-0.24	0.0132	0.0040		-8	-0.27	0.0126	0.0047		-2	-0.006	0.0109
	-1	-0.01	0.0130	0.0017		2	0.07	0.0123	0.0019		3	0.008	0.0109
	5	0.17	0.0131	0.0010		3	0.11	0.0125	0.0003		7	0.023	0.0111
	2.0	0.089	0.0154	0.0117		1.3	0.067	0.0141	0.0079		2.2	0.070	0.0131
	3.9	0.183	0.0229	0.0259		3.8	0.144	0.0206	0.0193		4.2	0.130	0.0196
	6.0	0.282	0.0389	0.0410		5.8	0.218	0.0319	0.0290		6.2	0.187	0.0218
	8.0	0.379	0.0604	0.0548		7.8	0.294	0.0495	0.0392		8.3	0.245	0.0281
	10.0	0.474	0.0892	0.0677		9.8	0.364	0.0711	0.0483		10.2	0.297	0.0328
	12.0	0.563	0.1251	0.0901		11.8	0.432	0.0975	0.0573		12.2	0.351	0.0376
	13.9	0.654	0.1659	0.0931		13.7	0.498	0.1278	0.0650		14.2	0.406	0.0404
	16.0	0.738	0.2131	0.1039		15.8	0.566	0.1645	0.0713		16.2	0.461	0.0427
	18.0	0.819	0.2661	0.1129		17.8	0.632	0.2057	0.0758		18.2	0.516	0.0451

TABLE III. - AERODYNAMIC CHARACTERISTICS OF CAMBERED WING AND SYMMETRICAL BODY; $R = 3.68 \times 10^6$

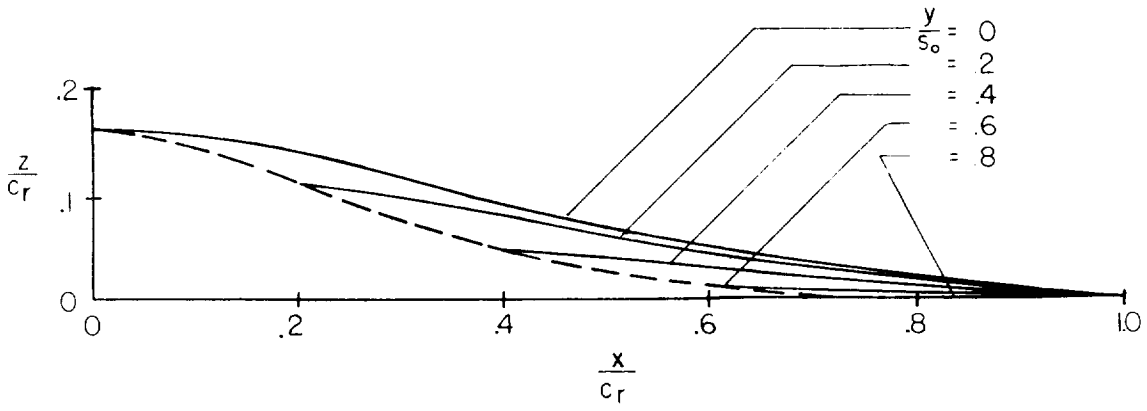
Transition wire on														
M	α	C_L	C_D	C_m	M	α	C_L	C_D	C_m	M	α	C_L	C_D	C_m
0.70	-10.7	-0.864	0.2329	0.0880	0.90	-10.6	-0.898	0.2334	0.1668	1.00	-10.4	-0.843	0.2380	0.1707
	-6.4	-5.30	1.292	0.777		-6.4	-6.59	1.415	1.282		-4.1	-5.13	0.976	1.245
	-4.3	-5.02	0.877	0.699		-4.2	-5.43	0.999	1.156		-2.0	-4.00	0.639	1.083
	-2.3	-3.80	0.569	0.611		-2.1	-4.04	0.620	0.890		1.1	-2.83	0.424	0.945
	-1.2	-2.64	0.341	0.541		2.0	-1.60	0.215	0.567		2.2	-1.68	0.264	0.794
	1.2	-1.43	0.200	0.473		4.1	-0.47	0.126	0.428		4.3	-0.49	0.186	0.591
	3.9	-0.48	0.132	0.401		6.2	0.57	0.119	0.341		6.4	0.59	0.175	0.438
	6.0	0.048	0.123	0.345		8.3	1.59	0.182	0.283		8.6	1.92	0.286	0.233
	8.1	1.139	0.165	0.306		10.5	2.80	0.358	0.226		10.6	3.23	0.476	0.027
	10.1	2.253	0.308	0.288		12.6	3.93	0.623	0.193		12.8	4.64	0.818	-0.166
	12.3	3.63	0.543	0.275		14.7	5.11	1.018	0.136		15.0	6.01	1.245	-0.365
	14.4	4.81	0.893	0.289		16.9	6.35	1.515	0.010		17.2	7.34	1.816	-0.565
	16.5	5.92	1.317	0.305		18.9	7.64	2.109	-0.073		19.2	8.44	2.394	-0.693
	18.6	7.00	1.840	0.304										

Transition wire off														
M	α	C_L	C_D	C_m	M	α	C_L	C_D	C_m	M	α	C_L	C_D	C_m
1.30	-10.5	-0.696	0.1948	0.1562	1.70	-10.5	-0.504	0.1446	0.1068	2.22	-10.0	-0.375	0.1070	0.0729
	-6.3	-4.96	1.083	1.226		-6.3	-4.98	1.083	1.226		-5.9	-2.88	0.609	0.599
	-4.2	-4.03	0.770	1.068		-4.2	-2.99	0.608	0.764		-3.8	-2.12	0.438	0.526
	2.1	-1.06	0.216	0.594		-2.2	-2.26	0.424	0.662		-1.8	-1.55	0.307	0.457
	4.2	-0.15	0.166	0.449		-1.1	-1.50	0.284	0.552		2.2	-0.96	0.211	0.382
	6.2	0.77	0.175	0.313		1.9	-0.74	0.199	0.443		2.3	-0.36	0.157	0.307
	8.5	1.84	0.255	0.167		4.0	0.01	0.163	0.338		4.3	0.23	0.147	0.235
	10.6	2.88	0.419	0.016		6.1	0.82	0.178	0.220		6.4	0.84	0.178	0.162
	12.7	3.93	0.685	-0.130		8.2	1.64	0.252	0.102		8.5	1.49	0.256	0.092
	14.9	4.99	1.046	-0.270		10.3	2.43	0.385	-0.004		10.6	2.09	0.374	0.040
	17.0	5.94	1.464	-0.392		12.5	3.23	0.594	-0.097		12.7	2.67	0.539	-0.008
	19.1	6.81	1.934	-0.493		14.5	3.97	0.857	-0.171		16.9	3.84	1.022	-0.044
						16.7	4.69	1.175	-0.236		18.9	4.38	1.317	-0.057
						18.7	5.38	1.550	-0.261					

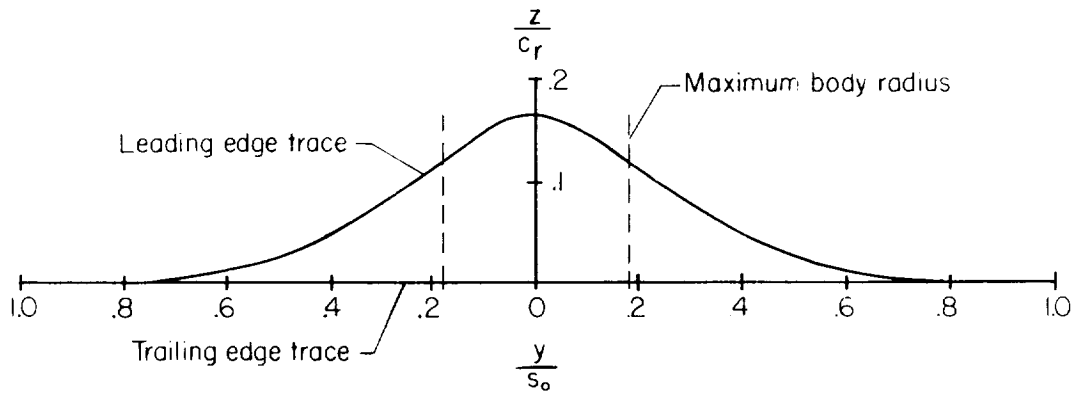
Transition wire off														
M	α	C_L	C_D	C_m	M	α	C_L	C_D	C_m	M	α	C_L	C_D	C_m
2.56	-0.4	-0.101	0.0206	0.0355	3.06	-0.4	-0.084	0.0198	0.0292	3.53	-0.4	-0.072	0.0215	0.0252
	-10.6	-3.49	1.021	0.648		-10.5	-3.01	0.908	0.523		-10.5	-2.68	0.434	0.434
	-6.5	-2.53	0.593	0.536		-6.5	-2.14	0.529	0.435		-6.5	-1.90	0.502	0.359
	-4.5	-2.05	0.432	0.478		-4.4	-1.71	0.389	0.389		-4.5	-1.50	0.369	0.323
	-2.5	-1.53	0.306	0.419		-2.4	-1.28	0.279	0.340		-2.5	-1.11	0.276	0.287
	-1.4	-1.01	0.208	0.358		-1.4	-0.84	0.197	0.296		-1.5	-0.73	0.200	0.253
	1.5	-0.48	0.153	0.294		1.5	-0.38	0.154	0.246		1.5	-0.34	0.162	0.219
	3.5	0.08	0.134	0.232		3.6	0.08	0.141	0.205		3.5	0.06	0.150	0.186
	7.6	0.96	0.182	0.063		7.6	1.98	0.420	0.090		7.6	0.90	0.215	0.143
	11.7	2.30	0.451	0.043		11.7	2.59	0.635	0.085		11.7	2.30	0.599	0.132
	14.3	2.99	0.694	0.025		14.4	3.29	0.855	0.085		14.3	2.30	0.599	0.132
	-1.4	-1.00	0.210	0.356		-1.4	-0.84	0.198	0.294		-1.4	-0.73	0.200	0.253

TABLE IV.- AERODYNAMIC CHARACTERISTICS OF SYMMETRICAL WING AND CAMBERED BODY; $R = 3.68 \times 10^6$

Transition wire on														
M	α	C_L	C_D	C_m	M	α	C_L	C_D	C_m	M	α	C_L	C_D	C_m
0.70	-16.9	-0.349	0.0491	0.0263	0.90	-16.8	-0.430	0.0637	0.0563	1.30	-16.7	-0.360	0.0618	0.0627
	-12.5	-.131	.0146	.0151		-12.4	-.133	.0161	.0208		-12.4	-.155	.0243	.0350
	-10.5	-.043	.0094	.0105		-10.3	-.032	.0104	.0120		-10.2	-.057	.0173	.0200
	-8.4	.051	.0080	.0057		-8.2	.071	.0099	.0039		-8.1	.041	.0163	.0057
	-6.3	.153	.0137	.0004		-6.0	.187	.0182	-.0062		-6.0	.146	.0225	-.0112
	-4.2	.261	.0280	-.0039		-3.9	.317	.0369	-.0185		-3.9	.251	.0367	-.0280
	-2.1	.378	.0513	-.0087		-1.7	.450	.0659	-.0323		-1.7	.356	.0593	-.0443
	-.5	.460	.0736	-.0112		-.2	.541	.0928	-.0411		-.2	.437	.0815	-.0569
	---	.493	.0832	-.0119		.3	.576	.1046	-.0446		.3	.467	.0903	-.0613
	.5	.519	.0916	-.0128		.8	.604	.1148	-.0476		.8	.489	.0986	-.0649
	2.1	.601	.1219	-.0154		2.5	.712	.1561	-.0649		2.3	.571	.1278	-.0774
	4.2	.724	.1738	-.0203		4.6	.833	.2133	-.0807		4.5	.662	.1716	-.0916
	6.3	.828	.2285	-.0206		6.7	.896	.2659	-.0757		6.6	.727	.2154	-.1022
	8.3	.897	.2828	-.0191		8.8	.990	.3326	-.0918		8.7	.813	.2726	-.1165
	10.4	.986	.3509	-.0251		10.9	1.059	.3983	-.0942		10.8	.866	.3219	-.1171
	12.5	1.066	.4241	-.0330		12.9	1.143	.4776	-.1164		12.9	.977	.4012	-.1425
M	α	C_L	C_D	C_m	M	α	C_L	C_D	C_m	M	α	C_L	C_D	C_m
1.70	-16.8	-0.276	0.0531	-0.0336	2.22	-16.5	-0.215	0.0437	-0.0106	0.0437	0.0106	0.0106	0.0437	0.0106
	-12.5	-.111	.0222	.0155		-12.2	-.083	.0196	.0016	.0196	.0016	.0016	.0196	.0016
	-10.4	-.033	.0168	.0058		-10.0	-.014	.0150	.0054	.0150	.0054	.0054	.0150	.0054
	-8.3	.050	.0167	-.0061		-8.0	.050	.0152	-.0124	.0152	-.0124	-.0124	.0152	-.0124
	-6.2	.129	.0219	-.0176		-5.9	.112	.0202	-.0198	.0202	-.0198	-.0198	.0202	-.0198
	-4.1	.205	.0325	-.0287		-3.8	.174	.0295	-.0270	.0295	-.0270	-.0270	.0295	-.0270
	-2.0	.281	.0490	-.0396		-1.7	.230	.0428	-.0336	.0428	-.0336	-.0336	.0428	-.0336
	-.5	.334	.0643	-.0469		-.2	.269	.0546	-.0383	.0546	-.0383	-.0383	.0546	-.0383
	---	.353	.0700	-.0494		.2	.285	.0597	-.0402	.0597	-.0402	-.0402	.0597	-.0402
	.5	.370	.0765	-.0515		.8	.297	.0644	-.0417	.0644	-.0417	-.0417	.0644	-.0417
	2.1	.422	.0973	-.0589		2.3	.337	.0807	-.0463	.0807	-.0463	-.0463	.0807	-.0463
	4.2	.485	.1275	-.0681		4.3	.386	.1042	-.0519	.1042	-.0519	-.0519	.1042	-.0519
	6.2	.551	.1634	-.0778		6.4	.439	.1326	-.0581	.1326	-.0581	-.0581	.1326	-.0581
	8.3	.615	.2043	-.0872		8.5	.491	.1659	-.0639	.1659	-.0639	-.0639	.1659	-.0639
	10.4	.676	.2498	-.0954		10.6	.542	.2029	-.0695	.2029	-.0695	-.0695	.2029	-.0695
	12.5	.728	.2967	-.0996		12.6	.591	.2430	-.0743	.2430	-.0743	-.0743	.2430	-.0743

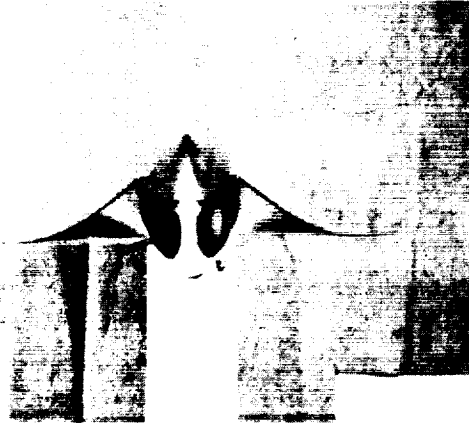


(a) Ordinates of mean-camber lines and leading edge.



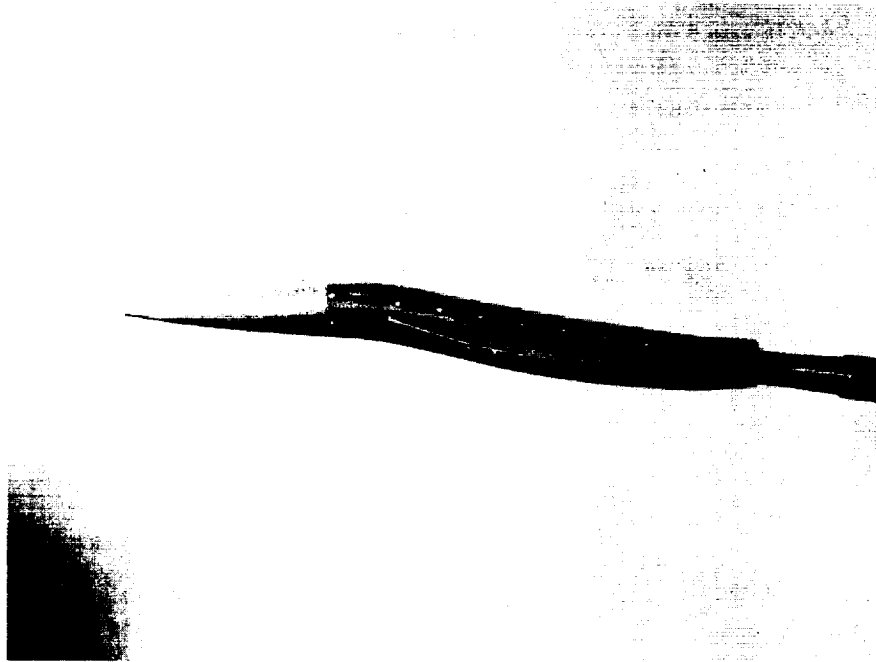
(b) Ordinates of leading- and trailing-edge traces.

Figure 1.- Wing mean surface shape.



A-23256

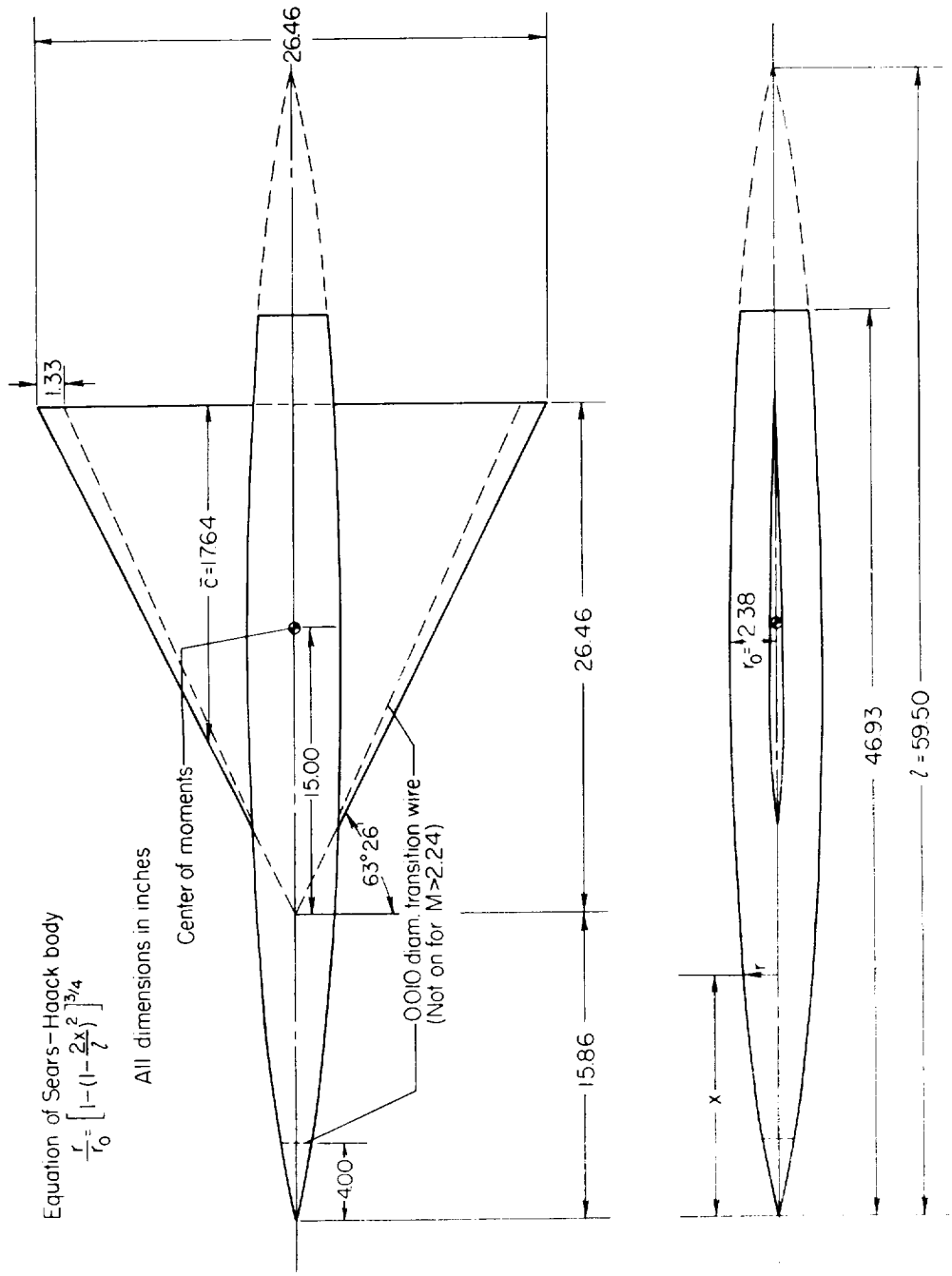
(a) Front view.



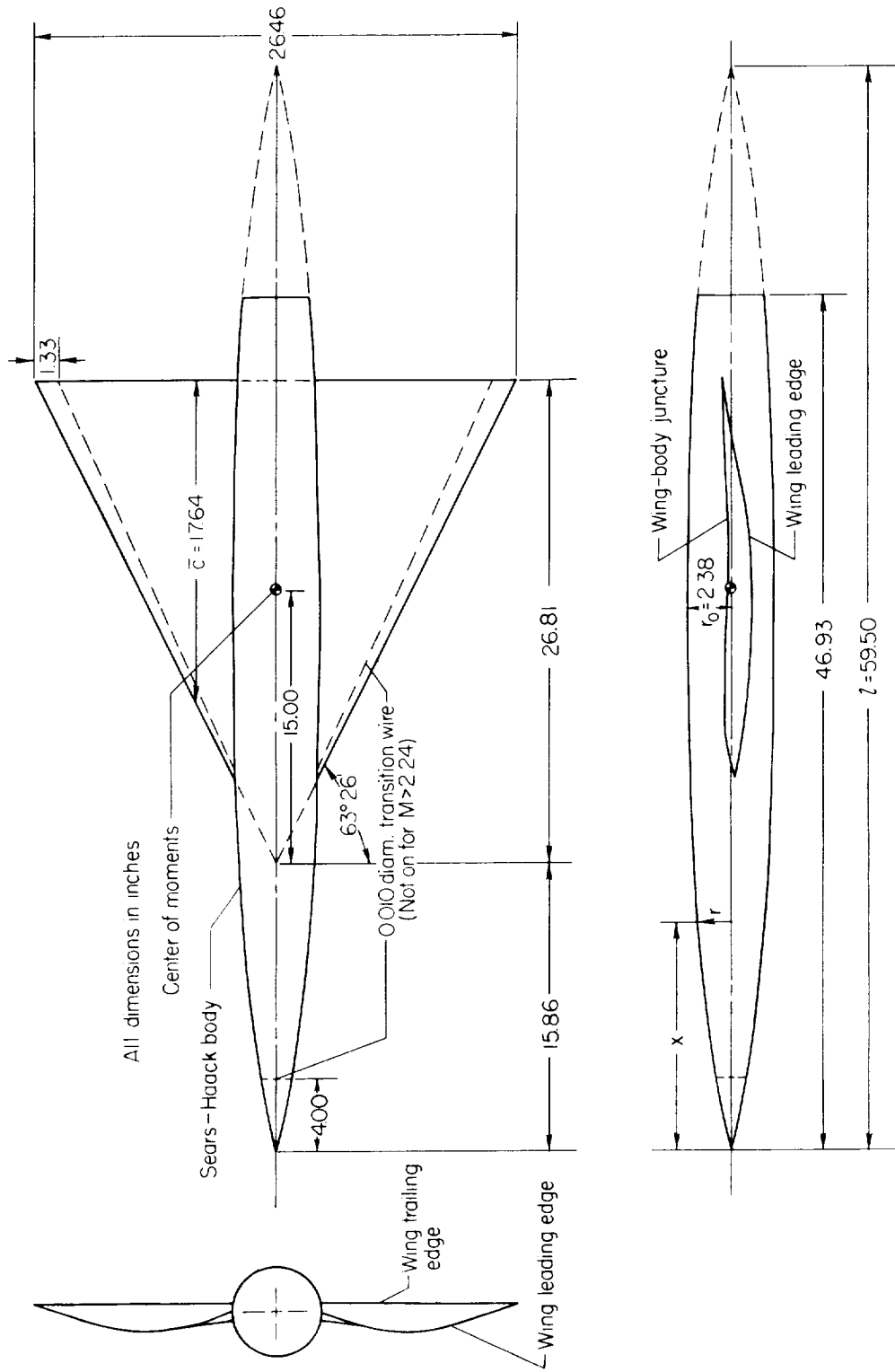
A-23257

(b) Side view.

Figure 2.- Photograph of cambered wing and cambered body model.

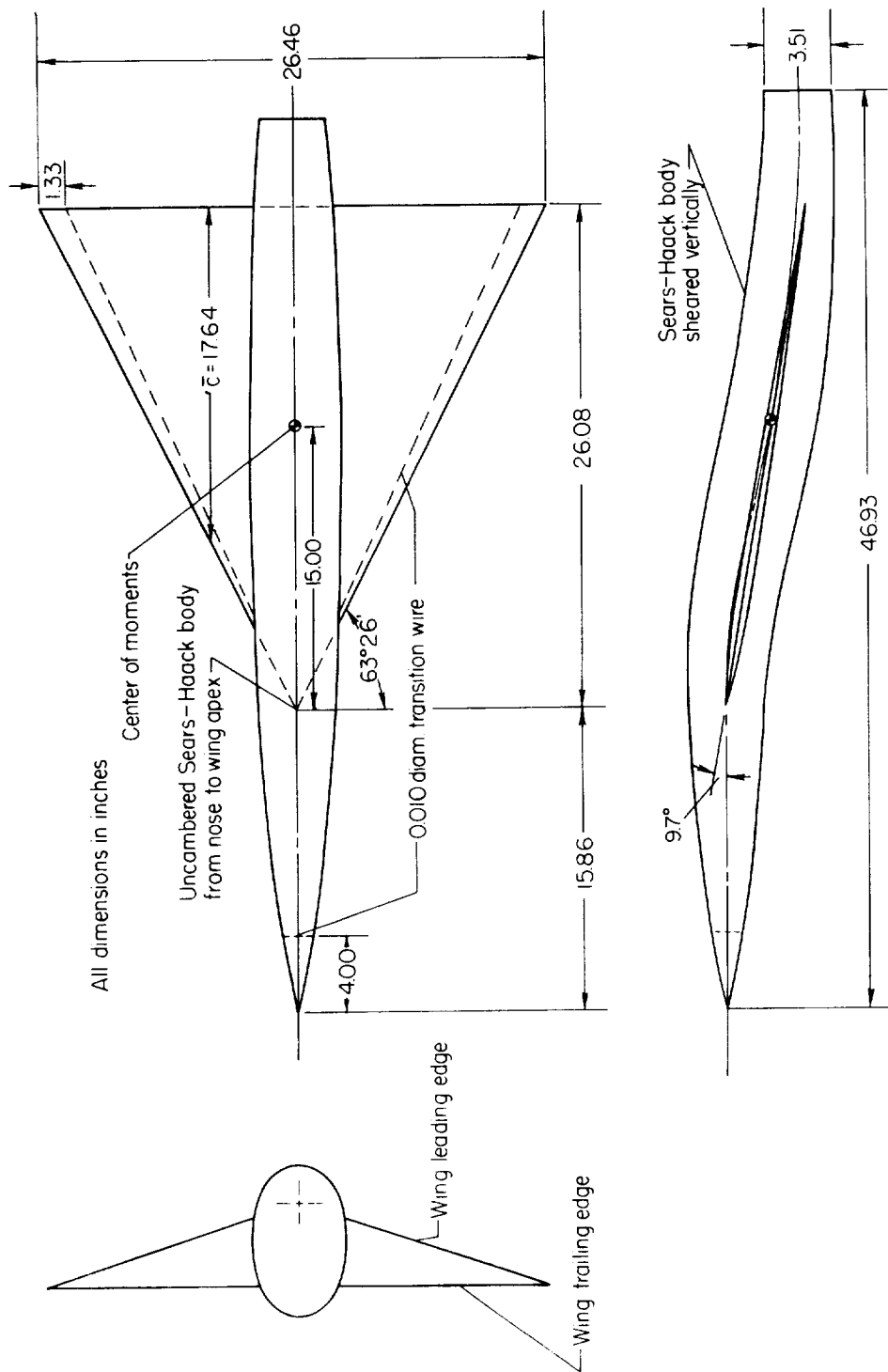


(a) Symmetrical wing and symmetrical body.
 Figure 3.- Dimensional sketches of models.



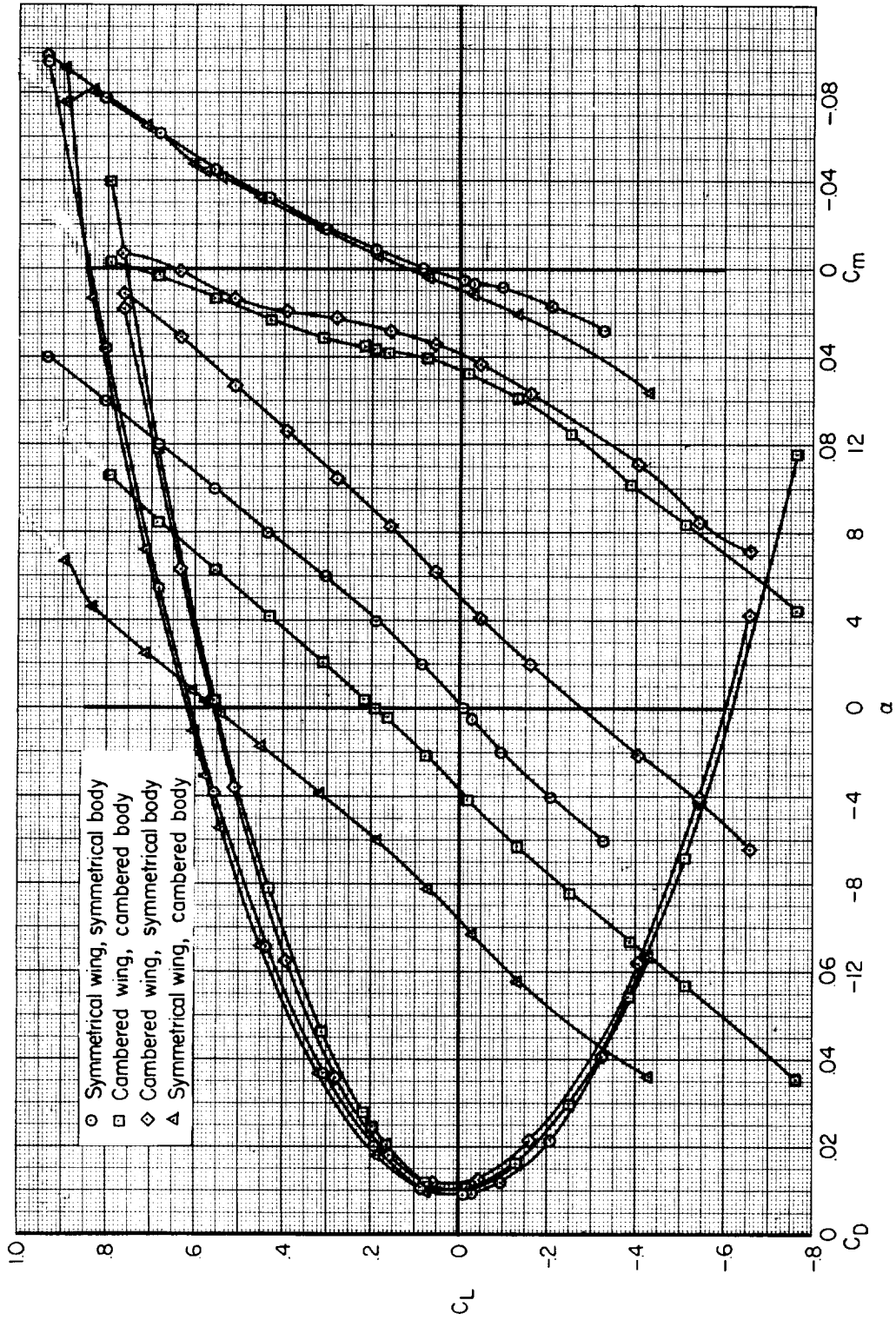
(c) Cambered wing and symmetrical body.

Figure 3.- Continued.



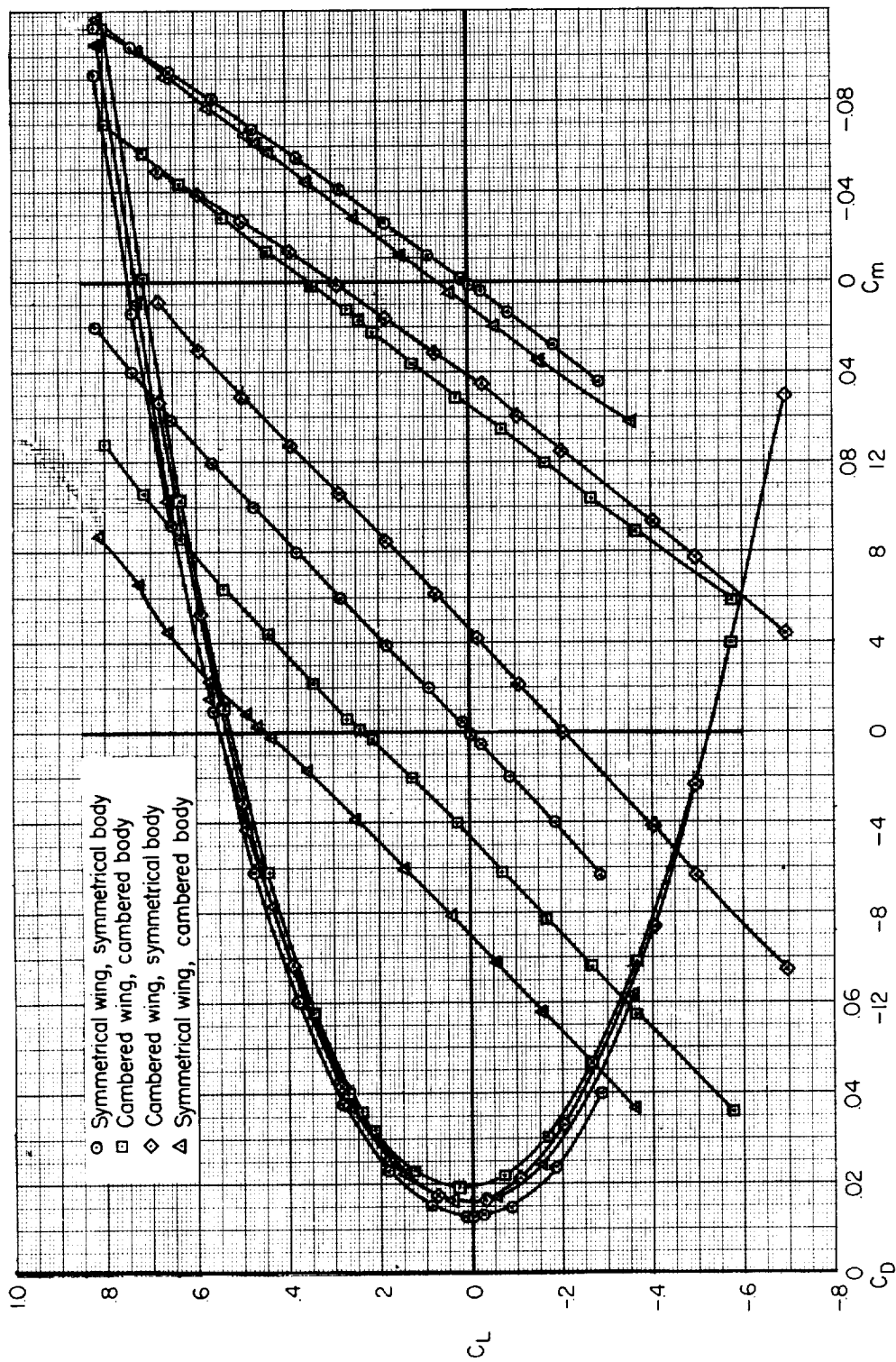
(d) Symmetrical wing and cambered body.

Figure 3.- Concluded.



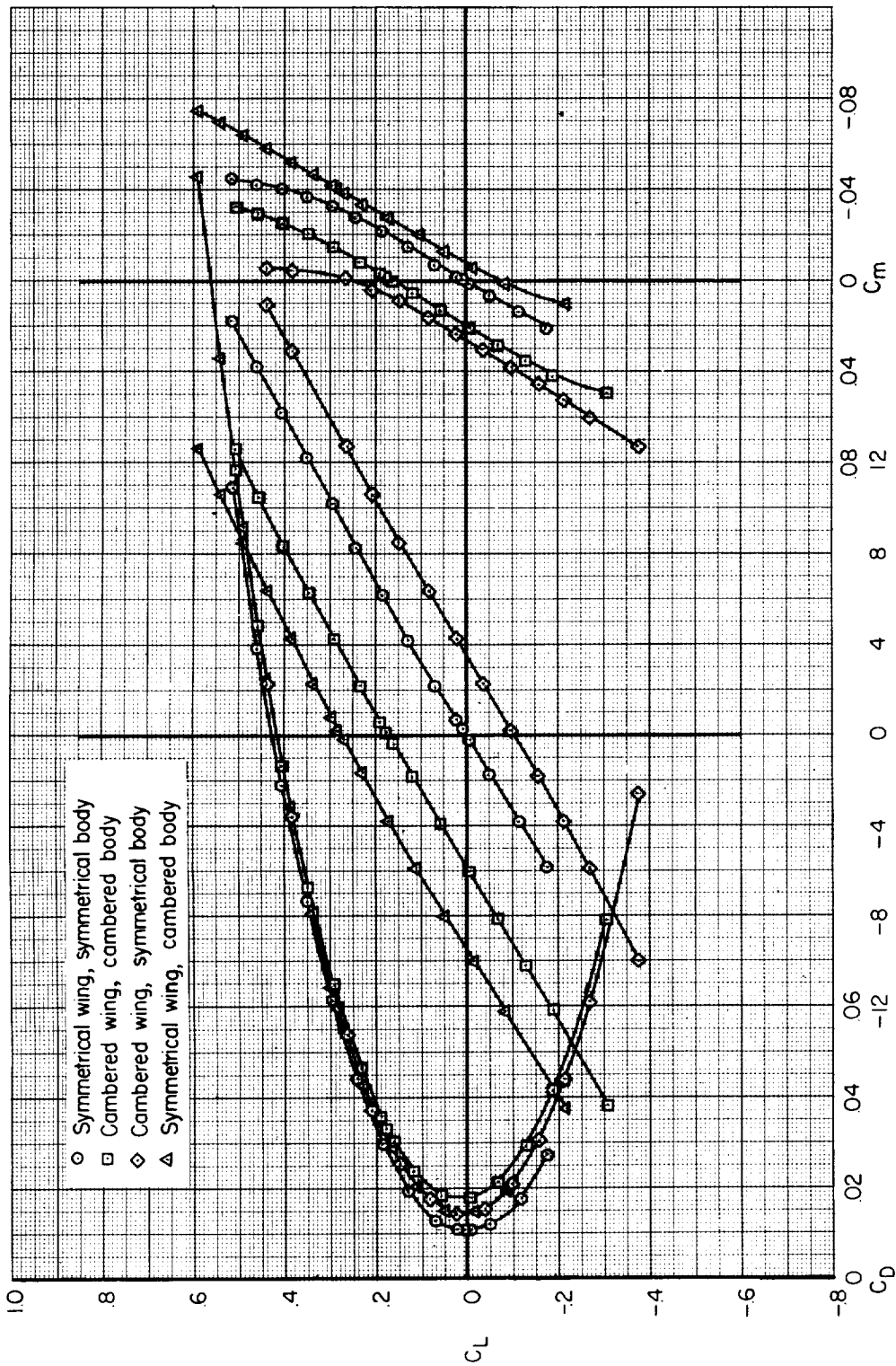
(a) $M = 0.90$

Figure 4.- Lift, drag, and pitching-moment characteristics.



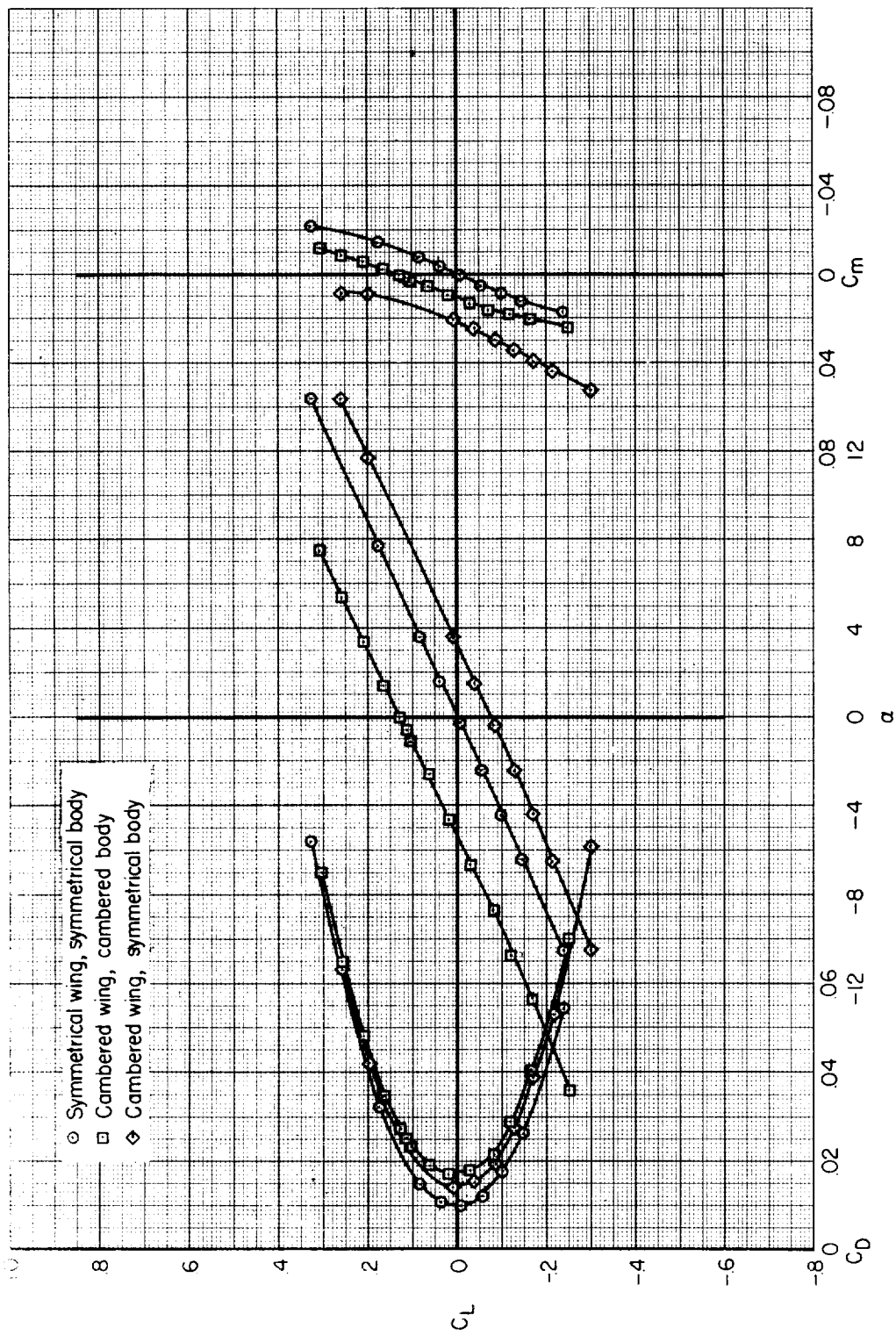
(b) $M = 1.30$

Figure 4.- Continued.



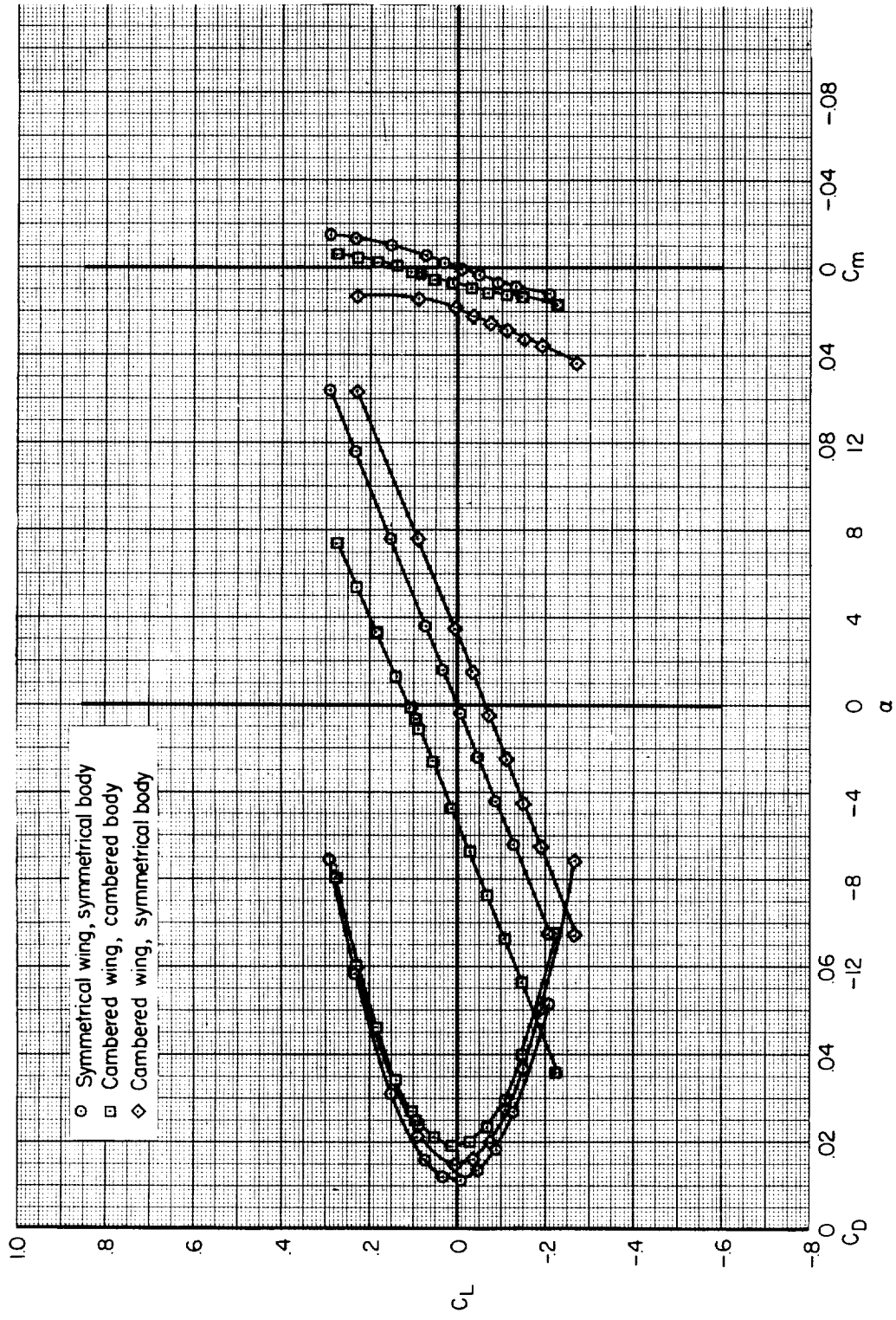
(c) $M = 2.22$

Figure 4.- Continued.



(d) $M = 3.06$

Figure 4.- Continued.



(e) $M = 3.53$

Figure 4.- Concluded.

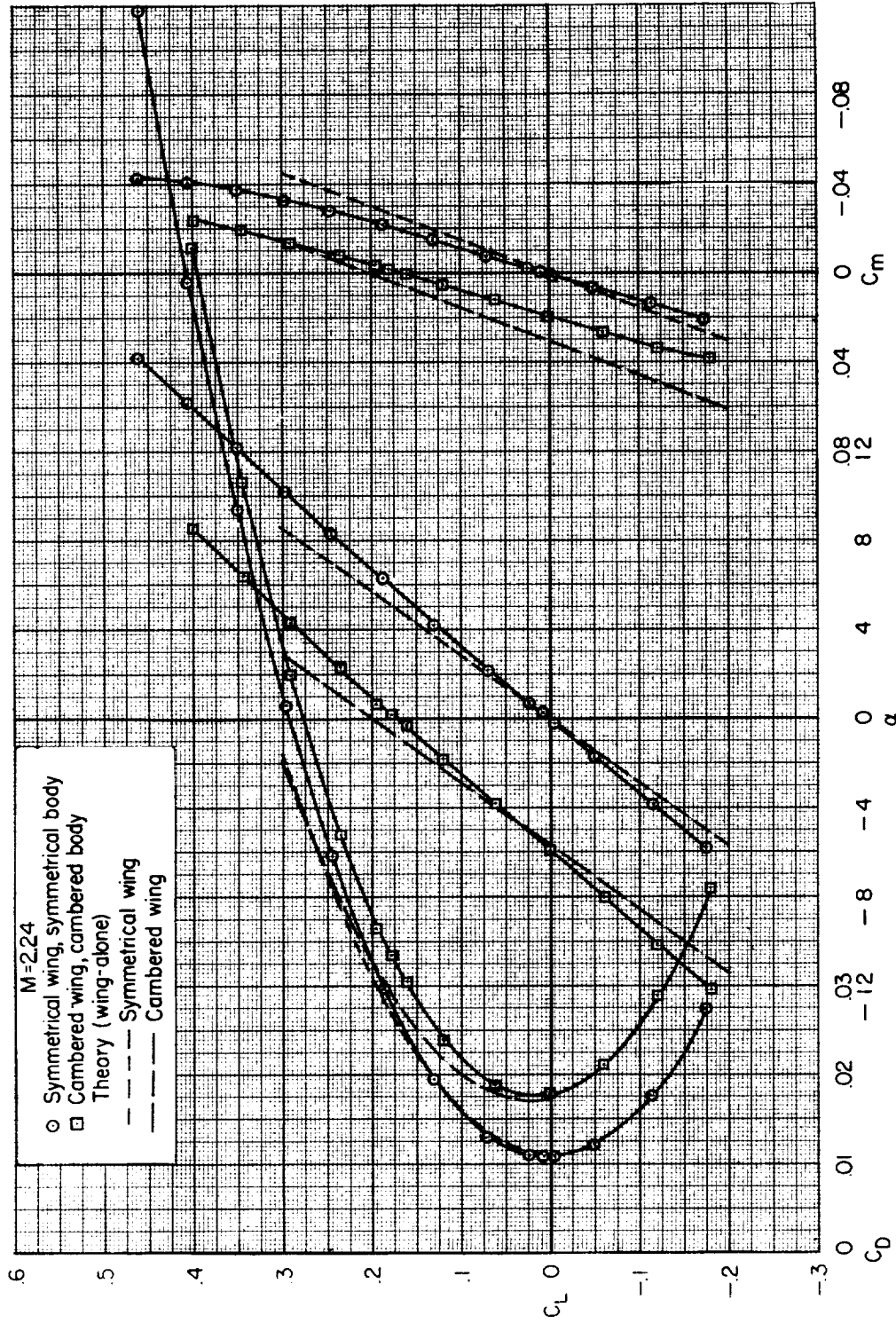


Figure 5.- A comparison of the theoretical and experimental characteristics at the design Mach number.

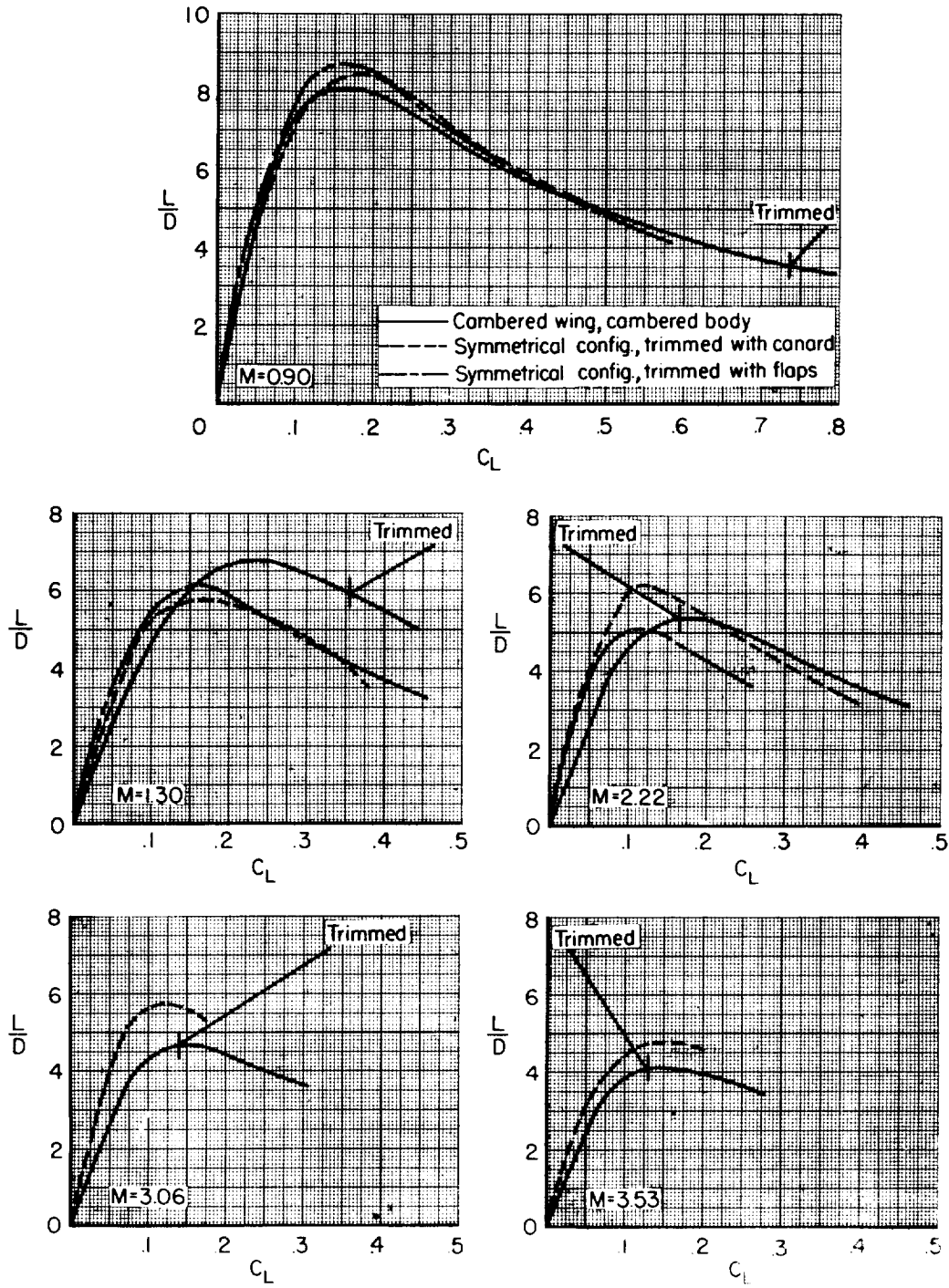


Figure 6.- A comparison of the lift-drag characteristics of the cambered wing and body with the symmetrical configuration trimmed with external controls.

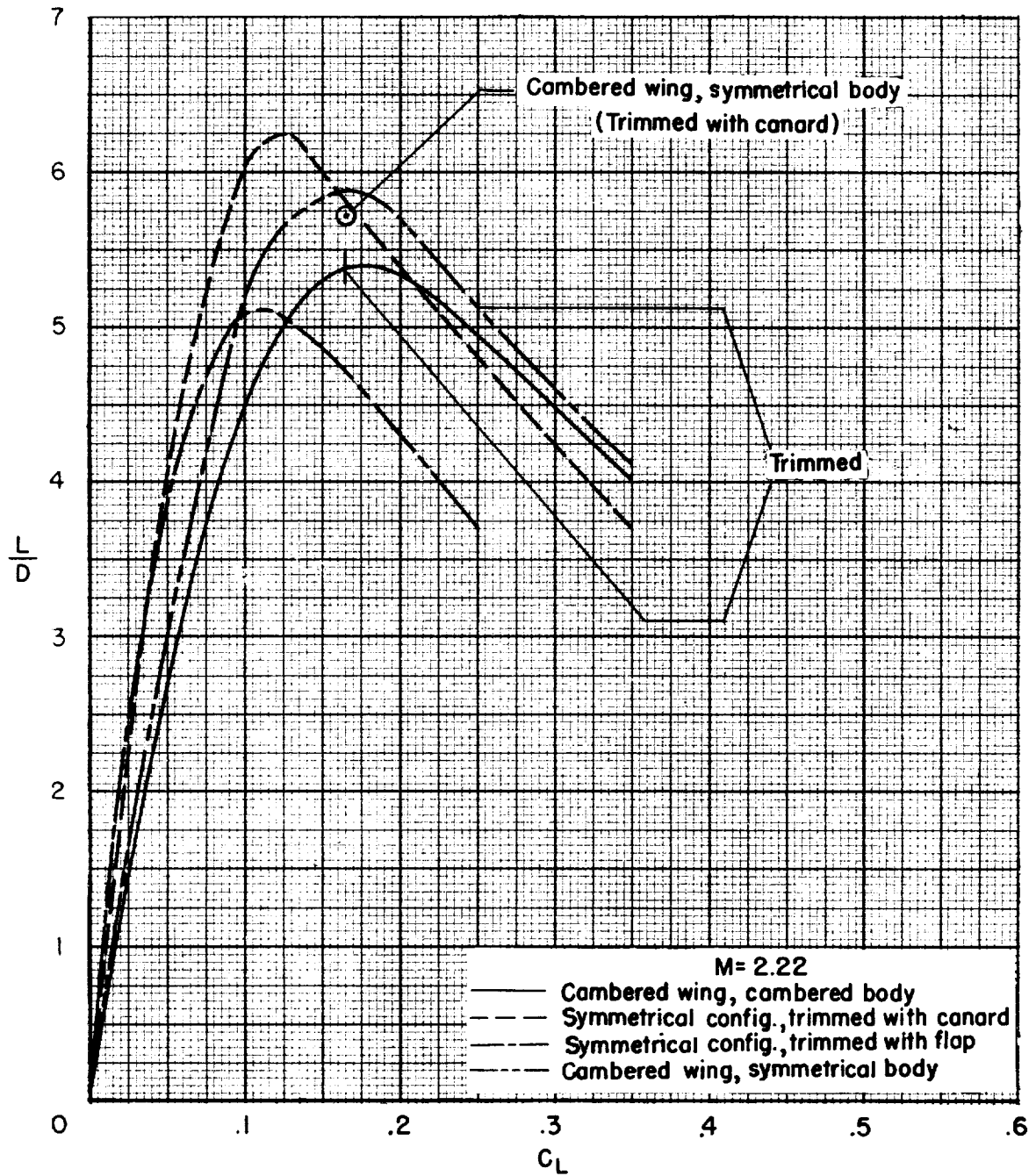


Figure 7.- Comparison of lift-drag characteristics at $M = 2.22$.

<p>NASA MEMO 2-3-59A National Aeronautics and Space Administration. AN EXPERIMENTAL INVESTIGATION OF A TRI- ANGULAR WING OF ASPECT RATIO 2 AND A BODY WARPED TO BE TRIMMED AT $M = 2.24$. Gaynor J. Adams and John W. Boyd. February 1959. 38p. diags., photos., tabs. (NASA MEMORANDUM 2-3-59A)</p> <p>Wing twist and camber and body camber were designed to reduce the drag due to lift at a trim lift coefficient of 0.2. The Mach number range of the tests was from 0.70 to 3.53, and the free-stream Reynolds number was 3.68 million, based on the wing mean aerodynamic chord. Other configurations tested were the warped wing in combination with a symmetrical body, a symmetrical wing on the cambered body, and a symmetrical wing on a symmetrical body.</p>	<p>1. Wing Sections - Camber (1.2.1.2.1) 2. Wings, Complete - Design Variables (1.2.2.2) 3. Mach Number Effects - Complete Wings (1.2.2.6) 4. Wing-Fuselage Combinations - Airplanes (1.7.1.1.1) I. Adams, Gaynor J. II. Boyd, John W. III. NASA MEMO 2-3-59A</p>	<p>NASA MEMO 2-3-59A National Aeronautics and Space Administration. AN EXPERIMENTAL INVESTIGATION OF A TRI- ANGULAR WING OF ASPECT RATIO 2 AND A BODY WARPED TO BE TRIMMED AT $M = 2.24$. Gaynor J. Adams and John W. Boyd. February 1959. 38p. diags., photos., tabs. (NASA MEMORANDUM 2-3-59A)</p> <p>Wing twist and camber and body camber were designed to reduce the drag due to lift at a trim lift coefficient of 0.2. The Mach number range of the tests was from 0.70 to 3.53, and the free-stream Reynolds number was 3.68 million, based on the wing mean aerodynamic chord. Other configurations tested were the warped wing in combination with a symmetrical body, a symmetrical wing on the cambered body, and a symmetrical wing on a symmetrical body.</p>	<p>1. Wing Sections - Camber (1.2.1.2.1) 2. Wings, Complete - Design Variables (1.2.2.2) 3. Mach Number Effects - Complete Wings (1.2.2.6) 4. Wing-Fuselage Combinations - Airplanes (1.7.1.1.1) I. Adams, Gaynor J. II. Boyd, John W. III. NASA MEMO 2-3-59A</p> <p>NASA</p>
<p>NASA MEMO 2-3-59A National Aeronautics and Space Administration. AN EXPERIMENTAL INVESTIGATION OF A TRI- ANGULAR WING OF ASPECT RATIO 2 AND A BODY WARPED TO BE TRIMMED AT $M = 2.24$. Gaynor J. Adams and John W. Boyd. February 1959. 38p. diags., photos., tabs. (NASA MEMORANDUM 2-3-59A)</p> <p>Wing twist and camber and body camber were designed to reduce the drag due to lift at a trim lift coefficient of 0.2. The Mach number range of the tests was from 0.70 to 3.53, and the free-stream Reynolds number was 3.68 million, based on the wing mean aerodynamic chord. Other configurations tested were the warped wing in combination with a symmetrical body, a symmetrical wing on the cambered body, and a symmetrical wing on a symmetrical body.</p>	<p>1. Wing Sections - Camber (1.2.1.2.1) 2. Wings, Complete - Design Variables (1.2.2.2) 3. Mach Number Effects - Complete Wings (1.2.2.6) 4. Wing-Fuselage Combinations - Airplanes (1.7.1.1.1) I. Adams, Gaynor J. II. Boyd, John W. III. NASA MEMO 2-3-59A</p>	<p>NASA MEMO 2-3-59A National Aeronautics and Space Administration. AN EXPERIMENTAL INVESTIGATION OF A TRI- ANGULAR WING OF ASPECT RATIO 2 AND A BODY WARPED TO BE TRIMMED AT $M = 2.24$. Gaynor J. Adams and John W. Boyd. February 1959. 38p. diags., photos., tabs. (NASA MEMORANDUM 2-3-59A)</p> <p>Wing twist and camber and body camber were designed to reduce the drag due to lift at a trim lift coefficient of 0.2. The Mach number range of the tests was from 0.70 to 3.53, and the free-stream Reynolds number was 3.68 million, based on the wing mean aerodynamic chord. Other configurations tested were the warped wing in combination with a symmetrical body, a symmetrical wing on the cambered body, and a symmetrical wing on a symmetrical body.</p>	<p>1. Wing Sections - Camber (1.2.1.2.1) 2. Wings, Complete - Design Variables (1.2.2.2) 3. Mach Number Effects - Complete Wings (1.2.2.6) 4. Wing-Fuselage Combinations - Airplanes (1.7.1.1.1) I. Adams, Gaynor J. II. Boyd, John W. III. NASA MEMO 2-3-59A</p> <p>NASA</p>

